

# A BRIEF REVIEW OF STRUCTURAL, ELECTRICAL AND ELECTROCHEMICAL PROPERTIES OF ZINC OXIDE NANOPARTICLES

Vandana Parihar, Mohan Raja and Rini Paulose

Centre for Advanced Materials Research, School of Engineering and Technology, Jagran Lakecity University, Mugaliyachap, Bhopal-462044, Madhya Pradesh, India

Received: August 01, 2018

**Abstract.** Nanotechnology allocate with the production and usage of material with nanoscale dimension, nanoparticles are large surface area to volume ratio and thus very specific properties. Zinc oxide (ZnO) nanoparticles had been in current studies due to its large bandwidth and high exciton binding energy and it has prospective applications such as electronic, optical, mechanical, magnetic and chemical properties that are significantly different from those of bulk counterpart. The aims of this review to provide a comprehensive view on structural, synthesis and electrochemical properties of the ZnO nanoparticles, which were synthesized by different methods.

## 1. INTRODUCTION

For last few years, among metal oxide nanoparticles, ZnO has been the subject of focused research due to their extraordinary electronic, optical, mechanical, magnetic and chemical properties that are significantly different from those of bulk counterpart [1]. Today, nanotechnology operates in various fields of science its operation for materials and devices using different techniques at nanometer scale. Nanoparticles are a part of nanomaterials that are defined as a single particle 1–100 nm in diameter [2]. Zinc oxide, with its unique physical and chemical properties, such as high chemical stability, high electrochemical coupling coefficient, broad range of radiation absorption, paramagnetic nature [3] and high photostability, is a multifunctional material. ZnO nanostructured materials have been received broad attention due to their famed performance in electronics, optics and photonics. ZnO is a key technological material. The lack of a centre of symmetry in wurtzite, combined with large electromechanical coupling, results in strong piezoelectric and

pyroelectric properties and the consequent use of ZnO in mechanical actuators and piezoelectric sensors. Along with, ZnO is a wide band-gap (3.37 eV) compound semiconductor that is suitable for various kinds of applications. They are: ultraviolet (UV) lasers, power generators, solar cells [4], gas sensors [5], field emission devices, capacitors, varistors, photocatalysts [6,7], transparent UV resistance coating, photoprinting, electrophotography, electrochemical and electromechanical nanodevices, sun screen lotion (cream), cosmetic wounds healing, anti-hemorrhoids, anti-bacterial agent [8], eczema and excoriation in the human medicine [9]. The powder ZnO is widely used as an additive in numerous materials and products including ceramics [10], glass, cement, rubber, lubricants, paints, ointments, adhesives, plastics, sealants, pigments, food (source of Zn nutrient), batteries, ferrites, and fire retardants [11]. ZnO based coating has been evaluated as a protective layer against moisture for wooden samples originating from coniferous (pine, fir) as well deciduous (beech, oak)

Corresponding author: M. Raja, e-mail: drmrja@jlu.edu.in

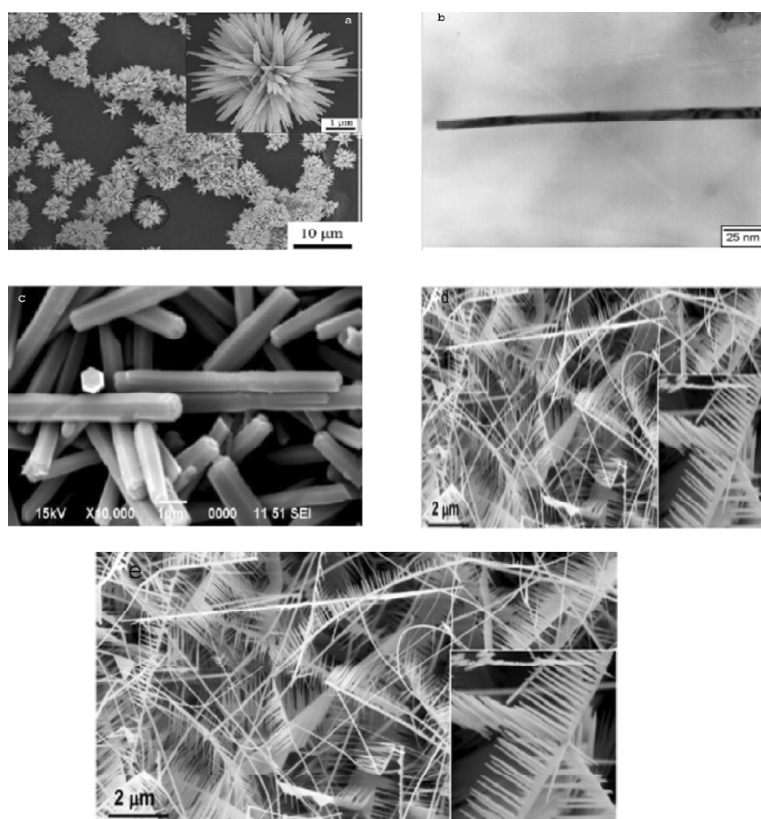


**Fig. 1.** Different shapes and structures of ZnO, (a) Flower, reprinted with permission from Ref [32], Copyright 2005 Elsevier, (b) Wire, reprinted with permission from Ref [33], copyright 2007 Elsevier, (c, d) Rod & Mushroom, reprinted with permission from (open access) Ref [34], copyright 2012 MDPI, (reprinted d) Comb with permission from Ref [35], Copyright 2003 American Physical Society.

trees [12]. ZnO nanoparticles distributed the manage of both physico chemical properties such as shape, size, surface area, crystal structure and dispensability. This has led to the development of a great variety of techniques for synthesizing the compound [13,]. Mechanochemical process [14,15], precipitation process [16,17], precipitation in the presence of surfactant [18], sol-gel [19], solvothermal, hydrothermal [20], microwave technique [21], emulsion [22], microemulsion method [23], chemical vapor deposition (CVD) [24], molecular beam epitaxy (MBE) [25], spray pyrolysis [26], pulse laser deposition [27], etc.

This review work is focused on structure and most important methods of preparation of ZnO divided into, chemical methods and as well as discussed about physical properties such as mechanical properties, electrical properties, Photoluminescence and electrochemical properties.

## 2. STRUCTURE OF ZnO

The structures of nanoscale zinc oxide means that ZnO can be classified among novel materials with

latent applications in numerous fields of nanotechnology [28,29]. Zinc oxide can arise in 1D, 2D, and three-dimensional (3D) structures. One-dimensional structures make up the leading group, including, needles, nanorods helices, rings and springs, ribbons, tubes, belts, combs and wires [30]. Zinc oxide can be obtained in 2D structures, such as nanosheet and nanoplate. Examples of 3D structures of zinc oxide contain flower, coniferous, snowflakes, urchin-like, dandelion etc. ZnO provides one of the greatest assortments of varied particle structures among all known materials [31], different shapes and structures of zinc oxide shown in Fig. 1. (a) Flower [32], (b) Wire [33], (c) Rod, Mushroom [34] and (d) Comb-like [35].

### 2.1. Crystal structure

Zinc oxide crystallizes in two main forms, hexagonal wurtzite and cubic zincblende. The wurtzite structure is most common and stable at ambient conditions. At ambient pressure and temperature, ZnO crystallized in the wurtzite (B4 type) structure shown in Fig. 2. This is a hexagonal lattice, belong-

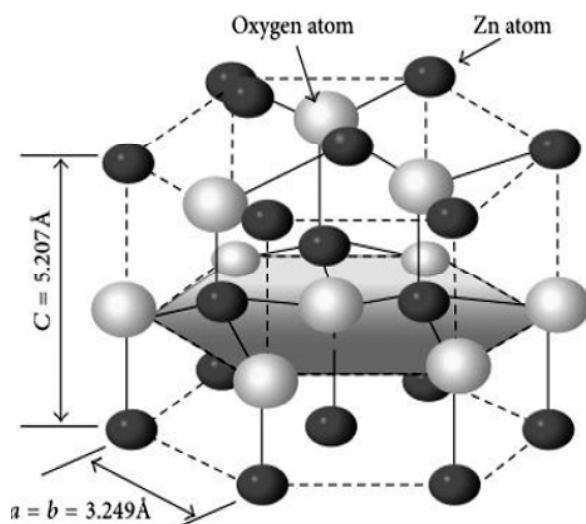


**Fig. 2.** Crystalline Structure of ZnO nanoparticles reprinted with permission from Ref [36], Copyright 2014 Hindawi.

ing to the space group P63mc, and is characterized by two interconnecting sublattices of  $\text{Zn}^{2+}$  and  $\text{O}^{2-}$ , such that each Zn ion is surrounded by tetrahedra of  $\text{O}^{2-}$  ions, and vice-versa. This tetrahedral coordination gives rise to polar symmetry along the hexagonal axis [36]. This polarity is responsible for a number of the properties of ZnO, including its piezoelectricity and spontaneous polarization, and is also a key factor in crystal growth, etching and defect generation. The four most common face terminations of wurtzite ZnO are the polar 'Zn' terminated (0001) and 'O' terminated (000.1) faces (c-axis oriented), and the non-polar (11.20) (a-axis) and (10.10) faces which mutually hold an equal number of Zn and 'O' atoms. The polar faces are known to possess different physical and chemical properties, and the 'O'-terminated face possesses a little different electronic structure to the other three faces 'O' [37].

### 3. METHODS OF SYNTHESIS OF ZINC OXIDE NANOPARTICLES

Synthesis of nanomaterials through a simple, low cost and in high yield has been a great face up to since the very before time progress of nanoscience. The techniques for synthesizing zinc nanoparticles can be separated into solid-phase, liquid-phase and gas-phase processes. The solid-phase techniques consist of mechanical ball milling and mechanochemical, the liquid-phase techniques include laser ablation, exploding wire, solution reduction, and decomposition process, while the gas-phase processes comprise gas evaporation, exploding wire, and laser ablation process, spark dis-

charges [38]. Chemical bath deposition (CBD) [39], green synthesis [7], wet-chemical method [40].

#### 3.1. Mechanochemistry

Mechanochemistry is the combination of chemical and mechanical occurrence on a molecular dimension and includes mechanical breakage and chemical show of mechanically strained solids. Mechanochemical synthesis differs from usual ball milling. A typical ball milling process beneath inert atmosphere results in a moderate reduction of powder particle size and ultimately the formation of nanosized grains within micron-sized particles. The mechanochemical routine involves the initiation of a solid-state displacement reaction during the ball milling process which can product in nanosized particles (down to ~5 nm in size) embedded within larger by-product phase particles [41]. The mechanochemical method was projected by Ao et al. They synthesized ZnO with a standard crystallite size of 21 nm. The milling process was carried out for 6 hrs, producing  $\text{ZnCO}_3$  where as the zinc oxide precursor. Calcination of the precursor at 600 °C formed ZnO with a hexagonal structure. Tests showed that the size of the ZnO crystallites depends on the milling time and calcination temperature. Increasing the milling time (2–6 h) led to a reduction in the crystallite sizes (21.5–25 nm), which may indicate the existence of a "critical moment". Meanwhile an increase in the calcination temperature from 400 to 800 °C caused an increase in crystallite size (18–35 nm) [14].

#### 3.2. Sol-gel synthesis

The sol-gel synthesis process of nanoparticles was released to form inorganic compound through chemical reaction of a certain solution. The benefits of using sol-gel method are that it generates a good rate of thermal stability, high mechanical stability, good solution resistance, and possibility to stimulate transformation.

Agustinaa et al. used sol-gel and calcinations method for the preparation of ZnO nanoparticles. Nano zinc oxides produced under these conditions were characterized based on crystal form, as well as the morphology and particle size. The outcome showed that the best process conditions for the synthesis of nano zinc oxide was recognized at ultrasonication time of 60 minutes and a pH of 10. The formed nano zinc oxide has a crystal size of 45.35 nm, more homogeneous morphology. The nano zinc oxide has a particle size of about 50 nm with a zinc oxide content of 87.31% [42].

### 3.3. Hydrothermal method

The hydrothermal method does not necessitate the use of organic solvents or supplementary processing of the product (grinding and calcination), which makes it a simple and environmentally friendly technique. This synthesis process takes place in an autoclave, where the mixture of substrates is heated slowly to a temperature of 100–300 °C and left for more than a few days. As a result of heating followed by cooling, crystal nuclei are formed, which then grow. This process has various advantages, counting the prospect of carrying out the synthesis at low temperatures, the different shapes and dimensions of the resulting crystals depending on the composition of the starting mixture and the process temperature and pressure,

Nehal A. Salahuddin and coworkers were prepared zinc oxide nanotubes by hydrothermal synthesis using zinc nitrate as a precursor. And they found length and average outer diameter of the ZnO nanotubes were about 2.4 μm and 200 nm, respectively [43].

### 3.4. Liquid-phase synthesis

Laser ablation Pulsed laser ablative deposition (PLD) is a striking synthetic method due to its ability to produce nanoparticles with a narrow size allocation and a low level of impurities. Three major steps to contribute in the laser ablation synthesis method and form of nanoparticles from an objective immersed in liquid. Yoshitake Masuda and coworkers found in their work Liquid phase morphology control of ZnO crystals was perceive with the simple aqueous solution method. ZnO nanowires were successfully created at 50 °C their size 50 μm in length and about 100 nm in width. The obtained nano wires have no branches and without aggregations [44].

### 3.5. Controlled precipitation

Controlled precipitation is a generally used method of obtaining zinc oxide, in view of the fact that it makes it achievable to acquire an outcome with repeatable properties. The process involves fast and spontaneous reduction of a solution of zinc salt using a reducing agent, to limit the growth of particles with specific dimensions, followed by precipitation of a precursor of ZnO from the solution. In the next phase this precursor undergoes thermal treatment, followed by milling to take away impurities. It is very complicated to break down the agglomerates that form, so the calcined powders have a high level of agglomeration of particles. The process of precipi-

tation is proscribed by parameters such as pH, temperature and time of precipitation.

Zinc oxide has also been precipitated from aqueous solutions of zinc chloride, zinc sulphate and zinc acetate in this process the concentration of the reagents, the rate of addition of substrates and the reaction temperature are controlling factor. Sadraei et al. used William-Hal method the obtained ZnO nanoparticles average size of 30 nm [45].

### 3.6. Vapor transport synthesis

The most common method to synthesize ZnO nanostructures utilizes a vapor transport process. It can be cauterized into the catalyst free vapor – solid (VS) process and catalyst – assisted vapor-liquid – solid (VLS) process it depends to difference on nano- structure formation mechanisms. VS process is naturally able to producing a wealthy range of nanostructure like nanowire , nanorods, nanobelts etc. In a typical VS process complex ZnO nanostructures such as nanohelices and nanobelts were synthesized by Kong et al and they found, as-prepared nanopartecles has a belt-shape with widths of 10-60 nm, thickness of 5-20 nm and lengths up to several hundreds of micrometers [46]. In such a process, Zn and oxygen or oxygen mixture vapor are ecstatic and react with each other, forming ZnO nanostructures. There are several ways to generate Zn and oxygen vapor. Decomposition of ZnO is a direct and simple method; however, it is limited to very high temperatures [47]. In the VS process, the nanostructures are fashioned by condensing directly from the vapor phase. Although various nanostructures can be obtained, this method noticeably provides less control on the geometry, alignment and precise location of ZnO nanostructures the geometrical parameters of this nanobelt are determined to be  $W$ 528 nm and  $T$ 519 nm. Table 1 summarizes the various methods of ZnO nanostructures manufacturing.

## 4. PHYSICAL PROPERTIES OF ZnO NANOSTRUCTURES

ZnO nanoparticles have marvelous physical properties. This is worth noting that as the dimension of semiconductor materials shrinks down continuously to nanometer or even smaller scale than in this reduction some of their physical properties undergo changes known as “quantum size effects.” For example, quantum confinement increases the band gap energy of quasi-one-dimensional (Q1D) ZnO, which has been confirmed by photoluminescence [48].

**Table 1.** Summary of methods of obtaining zinc oxide.

Method	Precursors	Synthesis conditions	Properties and applications	Ref
Mechanochemical 1 process	ZnCl <sub>2</sub> , Na <sub>2</sub> CO <sub>3</sub> , NaCl	calcination: 2 h, 600 °C	Hexagonal structure Particles diameter 21-25 nm	[14]
2 process		400-800 °C	Hexagonal structure Particle diameter 18-35nm	[15]
Precipitation process	Zn(NO <sub>3</sub> ) <sub>2</sub> , NaOH	synthesis: 2 h; drying: 2 h, 100 °C reaction: ~2 h, 25 °C; drying: 80 °C; calcination: 1 h, 350 °C	Particles of spherical size of around 40 nm	[16]
	ZnO powder, NH <sub>4</sub> HCO <sub>3</sub>		Hexagonal wurtzite structure; flower-like and rod-like shape ( <i>D</i> : 15-25 nm, BET: 50-70 m <sup>2</sup> /g)	[17]
Precipitation in the presence of surfactants	Zn(NO <sub>3</sub> ) <sub>2</sub> , NaOH, SDS, TEA (triethanolamine)	precipitation: 50 55 min, 101 °C	wurtzite structure, shape of rod-like ( <i>L</i> : 3.6 μm, <i>D</i> : 400 500 nm) shape of nut-like and rice-like, size: 1.2-1.5 μm	[18]
Sol - gel	Zn(CH <sub>3</sub> COO) <sub>2</sub> , oxalic acid, ethanol and methanol	reaction temperature: 60 °C; drying: 24 h, 80 °C; calcination: 500 °C	Zincite structure; aggregate particles: ~100 nm; shape of rod; particles <i>L</i> : ~500 nm, <i>D</i> : ~100 nm; BET: 53 m <sup>2</sup> /g	[19]
Solvothermal	Zn(CH <sub>3</sub> COO) <sub>2</sub> , Zn(NO <sub>3</sub> ) <sub>2</sub> , LiOH,	reaction: 10 48 h, 120 250 °C	hexagonal (wurtzite) structure, size of microcrystallites: 100 nm 20 μm	[20]
hydrothermal and microwave techniques	KOH, NH <sub>4</sub> OH ZnCl <sub>2</sub> , NaOH	reaction: 5 10 h, 100 220 °C in teflon-lined autoclave	particles morphology: bullet-like (100-200 nm), rod-like (100-200 nm), sheet (50-200 nm), polyhedron (200-400 nm), crushed stone-like (50-200 nm)	[21]
Emulsion	Zn(CH <sub>3</sub> COO) <sub>2</sub> , heptanes, Span-80, NH <sub>4</sub> OH	reaction: 1 h; aging: 2.5 h; drying: in rotary evaporator; calcination: 2 h, 700 1000 °C	hexagonal structure; spherical shape; particles diameter: 0.05-0.15 μm	[22]
Microemulsion	Zn(NO <sub>3</sub> ) <sub>2</sub> , NaOH, heptane, hexanol, Triton X-100, PEG400	reaction: 15 h, 140 °C; drying: 60 °C	hexagonal (wurtzite) structure; particles morphology: needle ( <i>L</i> : 150-200 nm, <i>D</i> : ~55 nm), nanocolumns ( <i>L</i> : 80 100 nm, <i>D</i> : 50-80 nm), spherical (~45 nm)	[23]

Accepting the elementary physical properties is crucial to the coherent design of functional devices. Exploration of the properties of individual ZnO nanostructures is necessary for developing their potential as the building blocks for prospect nanoscale devices. This review section will summarize the up-to-date research growth on the physical properties of ZnO nanostructures, including mechanical, electrical, magnetic and Photoluminescence properties [49].

#### 4.1. Mechanical properties

Direct measurement of the mechanical performance of individual nanostructures is quite challenging since the traditional measurement method for bulk material does not apply. Based on an electric-field-induced resonant excitation, Bai et al. characterized the bending modulus of ZnO nanobelts using TEM. In this method, a unique TEM sample holder was made to apply an oscillating electric field among a

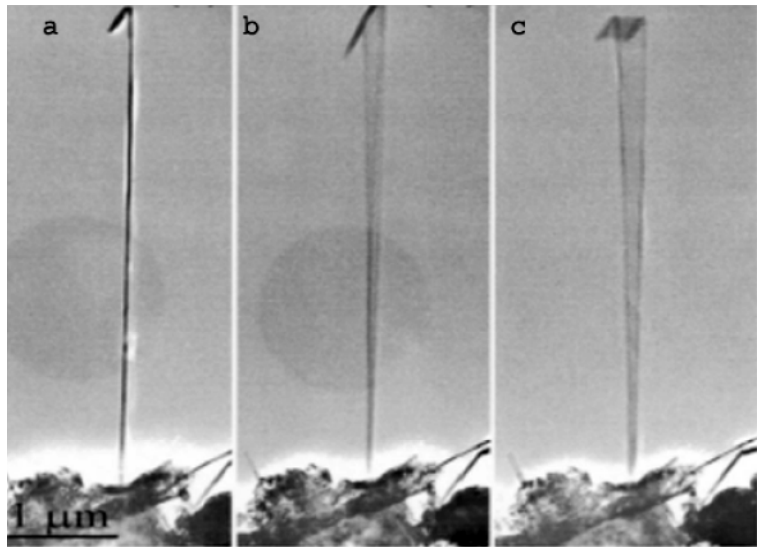


**Fig. 3.** A selected ZnO nanobelt with a hooked end at (a) stationary, (b) resonance at 731 kHz in the plane almost parallel to the viewing direction, and (c) resonance at 474 kHz in the plane closely perpendicular to the viewing direction, reprinted with permission from Ref [47], Copyright 2003 American Institute of Physics.

ZnO nanobelt and a fixed electrode. This electric field drove the shaking of the nanobelt, and resonant oscillation was gained as a result of tuning the driving frequency. Following the conventional elasticity theory, bending modulus was calculated. ZnO nanobelt demonstrates to be a promising material as nanoresonator and nanocantilever. Its small size renders improved sensitivity compared with conventional cantilever fabricated by microtechnology as shown in Fig. 3 [47]. Hughes et al. reported manipulation of the ZnO nanobelt to desired length and position. This shows the prospect of its application as a highly sensitive atomic force microscopy (AFM) cantilever [50].

## 4.2. Electrical properties

The fundamental revise of the electrical properties of ZnO nanoparticles is critical for raising their potential applications in nanoelectronics. Electrical transport measurements have been performed on the individual ZnO nanorods and nanowires [40,51]. Solitary ZnO nanowire was configured as a field effect transistor (FET) following numerous techniques. They were first dispersed in isopropanol alcohol to structure nanowire suspension and then deposited onto a  $\text{SiO}_2/\text{Si}$  substrate. Photolithography was utilized to characterize contact electrode range and degenerately doped Si substrate functioned as a back gate electrode. Due to the inhabitant defects such as oxygen vacancies and zinc interstitials, ZnO nanowires are reported to reveal n-type semiconductor behavior.

Chu and Li, worked on growth and electrical properties of doped ZnO by electrochemical deposition. They found that the electrical properties of ZnO were also dependent on the doping ions. In this work, only pure ZnO shows resistive switching behavior, demonstrating that the defects in ZnO is a key responsibility in inducing resistive switching behavior. In Fig. 4 (graph (a) case of pure ZnO), we can see a sudden drop of leakage of current indicating it having high resistance state and non volatile off state, while graphs (b) and (c) ( $\text{In}^{3+}$  and  $\text{Al}^{3+}$  doped ZnO, respectively) do not show resistance switching behavior by doping  $\text{Al}^{3+}$  conductivity has been increased and  $\text{In}^{3+}$  showed the rectifying behavior as current decrease on increasing voltage [52].

Madhuri et al. measured the electrical properties of ZnO and rGO-ZnO films were carried out as illustrated in Fig. 5a. Contacts were made by using an Ag paste over the films collected on  $\text{SiO}_2$  (300 nm)/Si substrates. The currents were measured in dark and light conditions by illuminating UV radiation externally ( $\lambda = 365 \text{ nm}$ ). I-V curves of ZnO are rectifying Schottky in nature due to metal/semiconductor contact as seen in Fig. 5b. At -1 V bias, the current in on state is nearly 7 times higher than that in off state. Fig. 5c, exhibits I-V curves obtained on rGO-ZnO hybrid films. The curves are slightly non-linear and rGO contact with ZnO brings about Schottky junctions aiding in the effectual charge transfer. Dark current observed for rGO-ZnO is nearly fifty times higher than ZnO. Although the increased value of current in off state is due to less resistive rGO film, the presence of ZnO is clearly exempli-

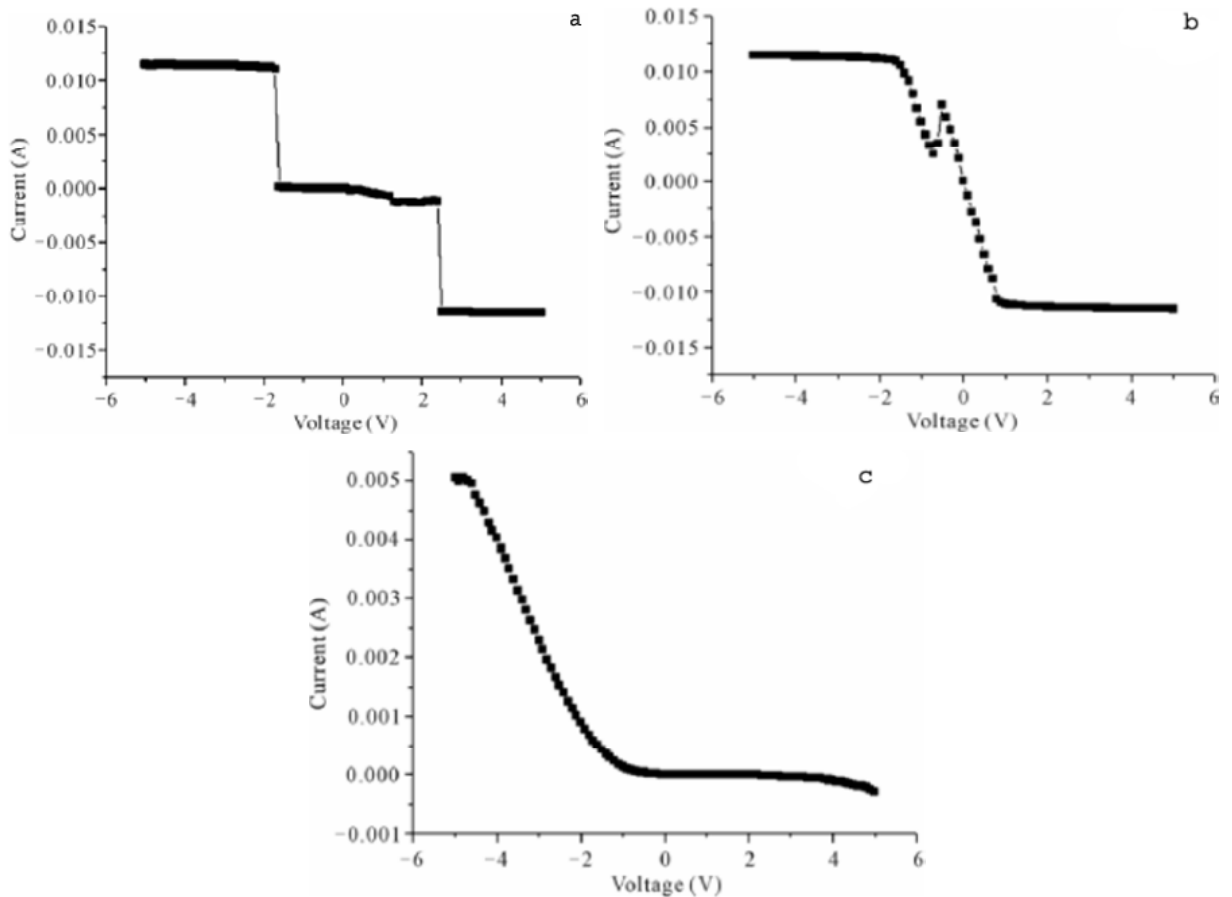


**Fig. 4.** Typical I-V characteristics of (a) Pure ZnO; (b) In<sup>3+</sup> doped ZnO; and (c) Al<sup>3+</sup> doped ZnO based on the FTO/ZnO/Pt structure, reprinted with permission from Ref [52], Copyright 2011 Scientific Research.

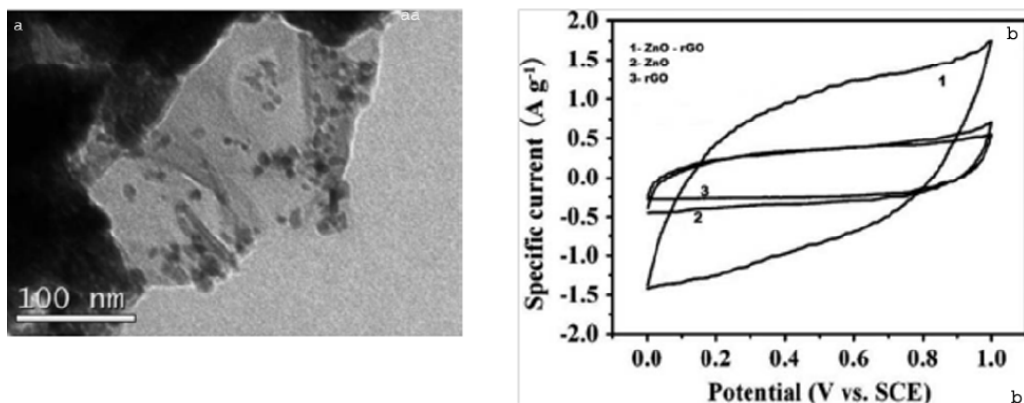


**Fig. 5.** (a) Schematic of the circuit for two-probe measurement; (b) and (c) I-V characteristics of the as synthesized films of ZnO NPs and rGO-ZnO NPs on SiO<sub>2</sub> with UV illumination on and off, reprinted with permission from Ref [53]. Copyright 2016 American Institute of Physics.

fied in UV-On conditions. In both the cases, we observed a linear increase in current with voltage [53].

**5. ELECTROCHEMICAL PROPERTIES**

The electrochemical properties of the nanostructured materials were investigated by galvanostatic cycling and cyclic voltammetry (CV). CV is a potentiodynamic electrochemical measurement,

where potential is measure between working electrode and the reference electrode by current is measured between working electrode and the counter electrode. Specific capacitance is calculated following [54,55] as:

$$C_s = \frac{Q}{\Delta V \times m} = \frac{I \times t}{\Delta V \times m},$$

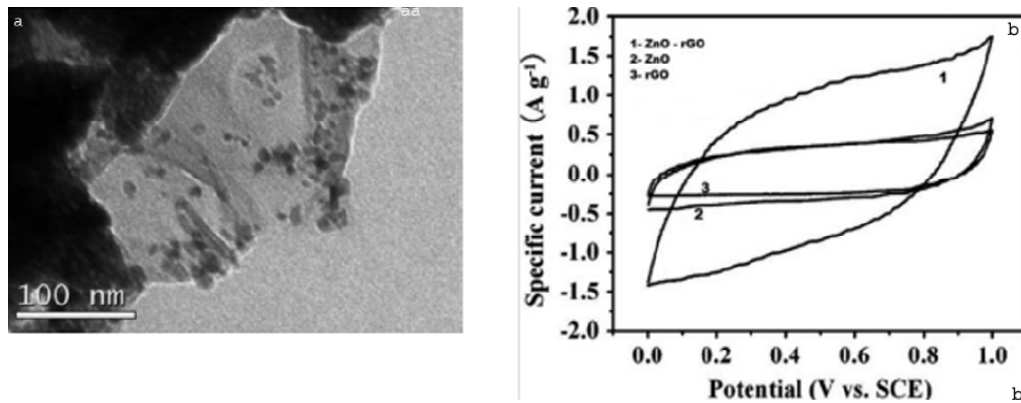


**Fig. 6.** (a) TEM images of ZnO/rGO composites, (b) The CV curves for ZnO, rGO, and the ZnO/rGO composite are electrodes in 0.1MNa<sub>2</sub>SO<sub>4</sub> electrolyte at the sweep rate of 5 mV/s, reprinted with permission of Ref. [56] Copyright 2014 Taylor & Francis.

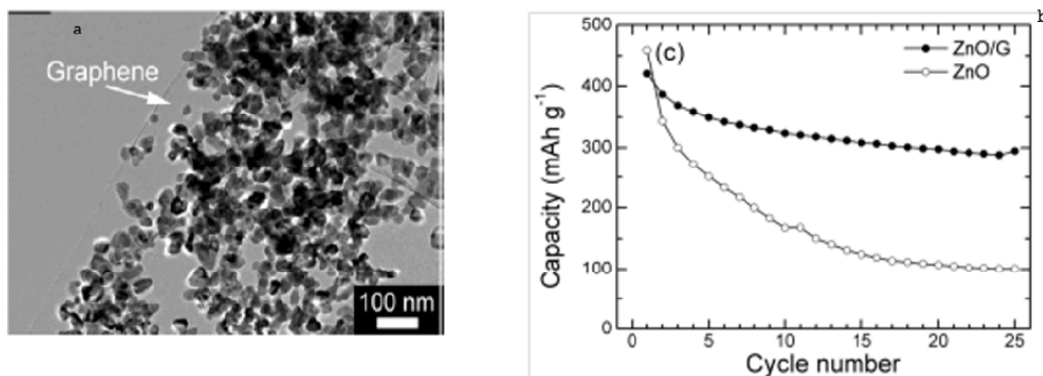


**Fig. 7.** (a) TEM image of ZnO/G and (b) comparison of cycling stability between bare ZnO and ZnO/G at 50 mA g<sup>-1</sup>, reprinted with permission (open access) of Ref [58], Copyright 2012 ESG.

where,  $C_s$  is specific capacitance of electrode,  $I$  is the current during the discharge process,  $t$  is the discharge time,  $\Delta V$  is potential window,  $m$  is the mass active electrode material.

Raja et al. prepared ZnO/rGO composite via wet chemical synthesis as shown in figure 6a, its CV curve showed a maximum integral area of positive synergetic effects in specific capacitance as shown in Fig.6 b. Its specific capacitance is 280 F/g which is far superior than pure ZnO and rGO at a current density of 1 A/g. [56].

K. S. Babu et al. observed in their electrochemical tests that the ZnO/graphene nanocomposite yields an initial charge capacity of 420 mAh g<sup>-1</sup>, and that the nanocomposite exhibits an obviously improved cycling stability compared to bare ZnO because of the buffering, confining and conducting effects of the incorporated graphene [57]. In Fig. 7, Song et al. prepared zinc oxide – graphene composite using in-situ hydrothermal synthesis, having a capacitance of 300 mAh g<sup>-1</sup> after 25 cycles, whereas pure ZnO dropped to 101 mAh g<sup>-1</sup> after same cycles. Incorporation of graphene enhanced the cyclic stability of pure ZnO [58].

Luo and co-workers prepared ZnO-SnO<sub>2</sub> composite by electrospinning method have shown improved cyclic performance at 700 °C due to smaller particle size of ZnO and SnO<sub>2</sub> as shown in Fig. 8 with a reversible capacity of 560 mAh g<sup>-1</sup> after 100 cycles whereas the composite calcined at 800 °C and 900 °C reduced in capacity after 100 cycles [59]

Guler et al. synthesised ZnO-MWCNTs have a capacity of 527 mAh g<sup>-1</sup> with superior cyclic stability upto 100 cycles shown in Fig. 9. This good stability was attributed to ZnO nanocrystals adhesion on CNT which have high electrical conductivity, excellent stress relaxation and good flexibility [60].

## 6. PHOTOLUMINESCENCE PROPERTIES OF ZnO

Rauwel et al. studied the photoluminescence properties of ZnO and carbon nanomaterials. ZnO presents the photoluminescence emission in the UV and visible section depending on the synthesis routes, size, shape, deep level, and surface defects. When ZnO nanoparticles pooled among carbon nanomaterials, it transforms of surface defects.

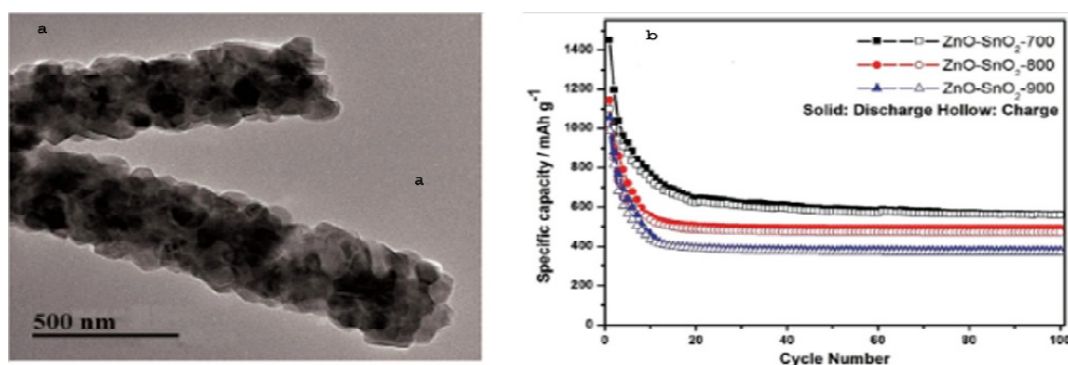


**Fig. 8.** (a) TEM images of ZnO–SnO<sub>2</sub> composite nanofibers. (b) Cycling performance and coulombic efficiencies, reprinted with permission of Ref [59], Copyright 2016 Elsevier.

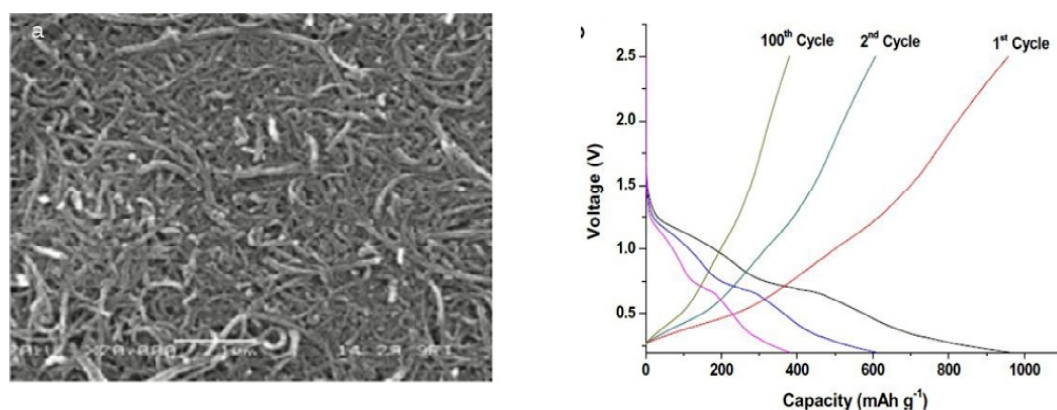


**Fig. 9.** (a) SEM and HRTEM images of the films oxidized under at high purity oxygen (99.999%) and argon (99.999%) in a ratio of (a) 1:4, (b) Galvanostatic charge–discharge curves of the films oxidized under (a) 1:4, (Oxygen:Argon) gas pressures, reprinted with permission of Ref [60], Copyright 2014 Elsevier.

Whereas ZnO allows regulation of these photoluminescence properties to produce, for example, white light. Moreover, efficient energy transfer from the ZnO to carbon nanostructures makes them appropriate candidates not only in energy harvesting applications, but as well in biosensors, photodetectors, and low temperature thermal imaging. Moreover, they have also shown that the embodiment of ZnO nanoparticles in a metal oxide matrix produces differences in the PL response due to the passivation of the surface defects [61]. Various colored emissions have been obtained for ZnO: orange, blue, green, and red [62].

## 7. APPLICATIONS OF ZnO NANOPARTICLES

Zinc oxide has diverse properties, both physical and chemical. It is widely used in many areas. ZnO plays an important role in a very wide range of applications, from pharmaceuticals to agriculture, tyres to ceramics, and from paints to chemicals. Fig. 10 shows the worldwide consumption of zinc oxide by region [63].

### 7.1. Medicinal uses

ZnO nanoparticles play some potential role in the CNS (*central nervous system*) and perhaps during development processes of diseases through mediating neuronal excitability or even release of neurotransmitters. Some studies have indicated that ZnO affected functions of different cells or tissues, biocompatibility, and neural tissue engineering [64].

### 7.2. Agriculture uses

Zinc oxide nanoparticles have prospective potential to boost the yield and growth of food crops. Seeds were treated with different concentrations of zinc oxide nanoparticles enhanced seed germination, seedling vigor, and plant growth and these zinc oxide nanoparticles also proved to be effective in increasing stem and root growth in seeds [65].

Paul and Ban, investigate the role of ZnO nanoparticles in the field of Biotechnology. They observed the effect of chemically synthesized Zinc oxide (ZnO) nanoparticles in biological system. When ZnO were applied at various concentrations

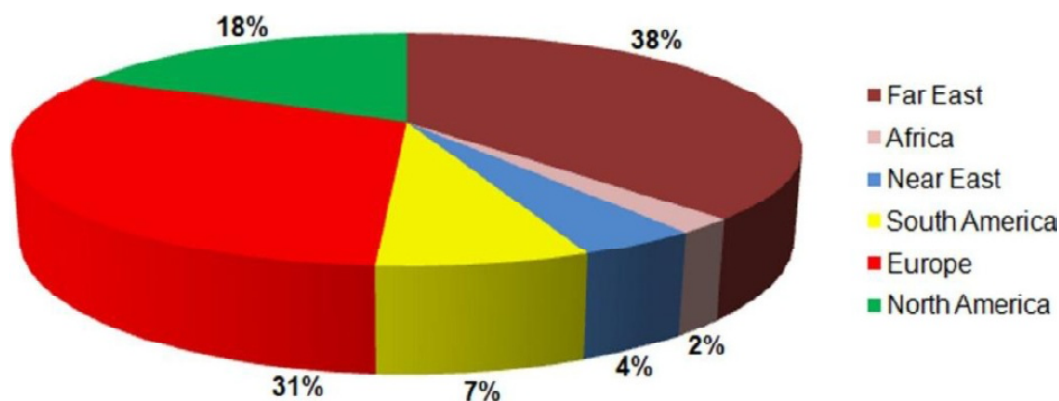


**Fig. 10.** Worldwide consumption of zinc oxide, reprinted with permission (open access) of Ref [63], Copyright 2014 MDPI.

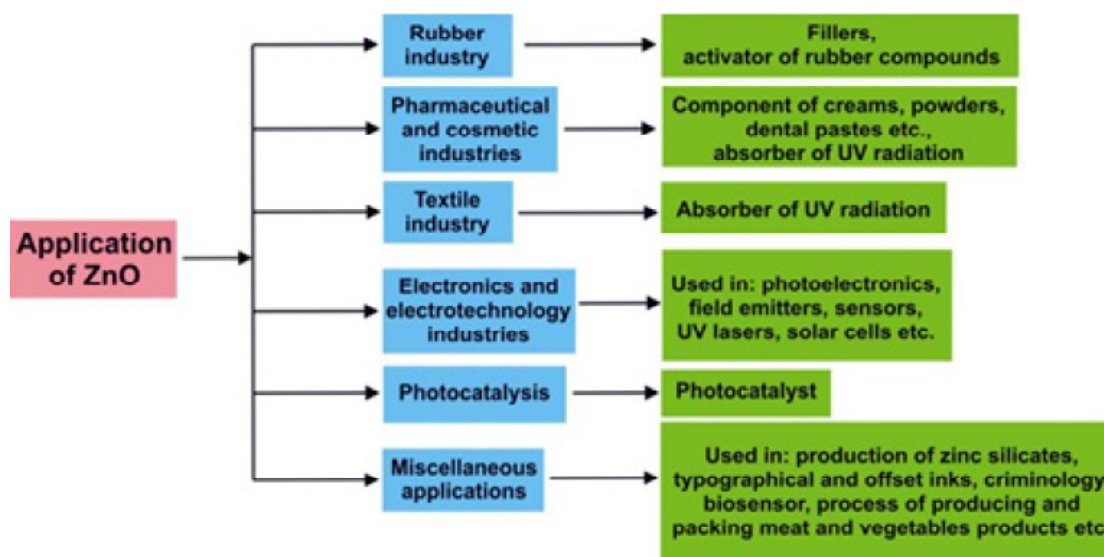


**Fig. 11.** Schematic representation all the application of ZnO mentioned in the text, reprinted with permission (open access) of Ref [63] Copyright 2014 MPDI.

in *Bacillus subtilis*, *Streptococcus pneumonia*, *Pseudomonas aeruginosa* and *E.Coli* cultures. It was found that a sharp increase in enzymatic activity with maxima at a ZnO concentration [66]. In summarizing form of zinc oxide applications in fields in Fig. 11 [63].

## 8. SUMMARY

Zinc oxide is a versatile, multifunctional and unique material because of its several properties thus ZnO offers incredible possibilities in future applications of electronic, optoelectronic, and magneto electronic devices. Encouraging progress on the research of nanostructured ZnO materials have been accomplished as reviewed in this article as well as focused on structure, synthesis and properties of ZnO nanoparticles. The addition of ZnO nanostructure building blocks for huge scale device applications is an additional important issue. Continuous effort

is committed to achieve great arrays of programmable structures for building reconfigurable architectures.

## ACKNOWLEDGEMENT

This work is supported by Department of Science and Technology (DST-SERB) India for the financial assistance under the scheme of Early Career Research (ECR) Award Ref: ECR/2015/000143.

## REFERENCES

- [1] H. Kumar and R. Rani // *International Letters of Chemistry, Physics and Astronomy* **14** (2013) 26.
- [2] R. Goyal and S. Bisnoi // *Indian J. Chem. Sec.* **51** (2012) 205.
- [3] S. Anuraj and C. Gopalakrishnan // *Nano-Structures & Nano-Objects* **11** (2017) 20.

- [4] W. Dongting, Z. Xuehong, F. Yuzhen, S. Jianhong, Z. Cong and Z. Xianxi // *Nano-Structures & Nano-Objects* **10** (2017) 1.
- [5] A. Tomchenko, A. Harmer, G.P. Marquis and B.T. Allen // *Sens. Actuators B* **93** (2003) 126.
- [6] G. Marcè, V. Augugliaro, López-Muñoz, M.J. Martín, C. Palmisano, L. Rives, V. Schiavello, M. Tilley and R.J.D. Venezia // *J. Phys. Chem. B* **105** (2001) 1033.
- [7] S. Singh, M. Joshi, P. Panthari, B. Malhotra, A.C. Kharkwal and H. Kharkwal // *Nano-Structures & Nano-Objects* **11** (2017) 1.
- [8] N. Serpone and D. Dondi // *Inorganica Chimica Acta* **360** (2007) 794.
- [9] U. Ozgur, D. Hofstetter and H. Morkoc // *Proceedings of the IEEE* **98** (2010) 1255.
- [10] S. Sabir, M. Arshad and S.K. Chaudhari // *The Scientific World Journal* **2014** (2014) 1.
- [11] N. Serpone and D. Dondi // *Inorganica Chimica Acta* **360** (2007) 794.
- [12] E. Makarona, C. Koutzagioti, C. Salmas, G. Ntalos, M.-Christina Skoulikidou and C. Tsamis // *Nano-Structures & Nano-Objects* **10** (2017) 57.
- [13] T.F. Melo and M.E. Jorge // *Mater. Lett.* **82** (2012) 13.
- [14] W. Ao, J. Li, H. Yang, X. Zeng and X. Ma // *Powder Technol.* **162** (2006) 128.
- [15] A. Stanković, L.J. Veselinović, S.D. Skapin, S. Marković and D. Uskoković // *J. Mater. Sci.* **46** (2011) 3716.
- [16] A.S. Lanje, S.J. Sharma, R.S. Ningthoujam and J.S. Ahn, R.B. Podes // *Adv. Powder Technol.* **24** (2013) 331.
- [17] Z.M. Khoshhesab, M. Sarfaraz and Z. Houshyar // *Synth. React. Inorg. Met. Org. Nano Met. Chem.* **42** (2012) 1363.
- [18] P. Li, Y. Wei, H. Liu and X.K. Wang // *J. Solid State Chem.* **178** (2005) 855.
- [19] T.H. Mahato, G.K. Prasad and B.S.J. Acharya // *J. Hazard. Mater.* **165** (2009) 928.
- [20] L.N. Dem yanets, L.E. Li and T.G. Uvarova // *J. Mater. Sci.* **41** (2006) 1439.
- [21] D. Chen, X. Cui and G. Cheng // *Solid State Commun.* **113** (2000) 363.
- [22] C.H. Lu and C.H. Yeh // *Mater. Lett.* **33** (1997) 129.
- [23] X. Li, G. He, G. Xiao, H. Liu and M. Wang // *J. Colloid Interface Sci.* **333** (2009) 465.
- [24] J.H. Park, S.J. Jang, S.S. Kim and B.T. Lee // *Appl. Phys. Lett.* **89** (2006) 121108.
- [25] P. Fons, H. Tampo, A.V. Kolobov, M. Ohkubo, S. Niki, J. Tominaga, R. Carboni and S. Friedrich // *Phys. Rev. Lett.* **96** (2006) 045504.
- [26] B. Josph, K.G. Gopchandran, P.V. Thomas, P. Koshy and V.K. Vaidyan // *Mater. Chem. Phys.* **58** (1999) 71.
- [27] J.J. Chen, M.H. Yu, W.L. Zhou and K. Sun // *Appl. Phys. Lett.* **87** (2005) 173119.
- [28] Y.B. Hahn // *Korean J. Chem. Eng.* **28** (2011) 1797.
- [29] Y. Ding, F. Zhang and Z. L. Wang // *Nano Research.* **6** (2013) 253.
- [30] T.F. Melo and M.E. Jorge // *Mater. Lett.* **82** (2012) 13.
- [31] A. K. Radzimska and T. Jesionowski // *Materials* **7** (2014) 2833.
- [32] Q. Xie, Z. Dai, J. Liang, L. Xu and W. Yu // *Solid State Commun.* **136** (2005) 304.
- [33] W.J. Chen, W.J. Liu and S.H. Hsieh // *Appl. Surf. Sci.* **253** (2007) 6749.
- [34] I. U. Haq // *Sensors (Basel)* **12** (2012) 8259.
- [35] Z. L. Wang, X. Y. Kong and J. M. Zuo // *Phys. Rev. Lett.* **91** (2003) 1.
- [36] S. Sabir, M. Arshad and S. K. Chaudhari // *The Scientific World Journal* **2014** (2014) 1.
- [37] O. Dulub, L.A. Boatner and U. Diebold // *Surf. Sci.* **519** (2002) 201.
- [38] H. Kabbara, J. Ghanbaja, C. Noël and T. Belmonte // *Nano-Structures & Nano-Objects* **10** (2017) 22.
- [39] V. Manthina and A. G. Agrios // *Nano-Structures & Nano-Objects* **7** (2016) 1.
- [40] R.N. Gayen and R. Paul // *Nano-Structures & Nano-Objects* (2016), doi.org/10.1016/j.nanoso.2016.03.007.
- [41] H. R. Ghorbani // *Orient. J. Chem.* **30** (2014) 1941.
- [42] S. Agustina, N. S. Indrasti, Suprihatin and N. T. Rohman // *International Journal of Sciences Basic and Applied Research* **22** (2015) 151.
- [43] A. Nehal, M. Salahuddin, I. El-Kemary and M. Ebtisam // *International Journal of Scientific and Research Publications* **5** (2015) 1.
- [44] Y. Masuda, N. Kinoshita and K. Koumoto // *ISRN Nanotechnology* **2012** (2012) 1.
- [45] R. Sadraei // *Journal of Chemistry* **5** (2016) 45.
- [46] X.Y. Kong and Z.L. Wang // *Nano Letters* **3** (2003) 1625.
- [47] X. D. Bai, P. X. Gao, Z. L. Wang and E. G. Wang // *Appl. Phys. Lett.* **82** (2003) 4806.

- [48] Z. L. Wang and X. Y. Kong // *Phys. Rev. Lett.* **91** (2003) 1.
- [49] L. M. Kukreja, S. Barik and P. Misra // *Cryst. Growth* **268** (2004) 531.
- [50] W. L. Hughes and Z. L. Wang // *Appl. Phys. Lett.* **82** (2003) 2886.
- [51] W. I. Park, J. S. Kim, G.C. Yi, M. H. Bae and H.J. Lee // *Appl. Phys. Lett.* **85** (2004) 52.
- [52] D. Chu and S. Li. // *New Journal of Glass and Ceramics* **2** (2012) 13.
- [53] K. P. Madhuri, K. Bramhaiah and N. S. John // *AIP Conference Proceedings* **1731** (2016) 050094.
- [54] Y.G. Wang and X.G. Zhang // *Electro. Chem. Acta* **49** (2004) 1957.
- [55] J. Gamby, P.L. Taberna, P. Simon, J.P. Fauvarque and M. Chesneau // *J. Power Sources* **101** (2001) 109.
- [56] M. Raja, A.B.V. Kiran Kumar, N Arora and J. Subha // *Nanotubes and Carbon Nanostructures* **234** (2015) 691.
- [57] K. S. Babu and V. Narayanan // *Chem Sci Trans.* **2** (2013) S33.
- [58] W. Song, J. Xie, S. Liu, Y. Zheng, G. Cao, T. Zhu and X. Zhao // *Int. J. Electrochem. Sci.* **7** (2012) 2164.
- [59] L. Luo, W. Xu, Z. Xia, Y. Fei, J. Zhu, C. Chen, Y. Lu, Q. Wei, H. Qiao and X. Zhang // *J. Ceram. Int.* **42** (2016) 10826.
- [60] M.O. Guler, T. Cetinkaya, U. Tocoglu and H. Akbulut // *Eng.* **118** (2014) 54.
- [61] P. Rauwel, M. Salumaa, A. Aasna, A. Galeckas and E. Rauwel // *J. Nanomater.* **2016** (2016) 1.
- [62] A. El Hichou, M. Addou, J. Ebothé and M. Troyon // *J. Lumin.* **113** (2015) 183.
- [63] A. K. Radzimska and T. Jesionowski // *Materials* **7** (2014) 2833.
- [64] M.J. Osmond and M. J. McCall // *Nanotoxicology* **4** (2010) 15
- [65] T.N.V.K.V. Prasad, P. Sudhakar and Y. Sreenivasulu // *Journal of Plant Nutrition* **35** (2012) 905.
- [66] S.Paul and D. K. Ban // *Int. Journal of Advances in Chemical Engg. & Biological Sciences* **1** (2014) 2349.